

Continuously tunable optical buffer with a dual silicon waveguide design

Peter Horak,^{*} Will Stewart, and Wei H. Loh

Optoelectronics Research Centre, University of Southampton, Southampton SO17 1BJ, UK
^{*}peh@orc.soton.ac.uk

Abstract: We propose a design for an optical buffer that comprises two coupled silicon waveguides, which is capable of generating a large continuously tunable change in the propagation delay time. The optical delay can be varied by more than 100% through varying the spacing between the waveguides.

©2011 Optical Society of America

OCIS codes: (200.4490) Optical buffers; (230.4685) Optical microelectromechanical devices; (130.0130) Integrated optics.

References and links

1. R. Langenhorst, M. Eiselt, W. Pieper, G. Grosskopf, R. Ludwig, L. Kuller, E. Dietrich, and H. G. Weber, "Fiber loop optical buffer," *J. Lightwave Technol.* **14**(3), 324–335 (1996).
 2. H. Park, J. P. Mack, D. J. Blumenthal, and J. E. Bowers, "An integrated recirculating optical buffer," *Opt. Express* **16**(15), 11124–11131 (2008).
 3. F. Xia, L. Sekaric, and Y. Vlasov, "Ultracompact optical buffers on a silicon chip," *Nat. Photonics* **1**(1), 65–71 (2007).
 4. J. Yang, N. K. Fontaine, Z. Pan, A. O. Karalar, S. S. Djordjevic, C. Yang, W. Chen, S. Chu, B. E. Little, and S. J. B. Yoo, "Continuously tunable, wavelength-selective buffering in optical packet switching networks," *IEEE Photon. Technol. Lett.* **20**(12), 1030–1032 (2008).
 5. J. B. Khurgin, "Optical buffers based on slow light in electromagnetically induced transparent media and coupled resonant structures: a comparative analysis," *J. Opt. Soc. Am. B* **22**(5), 1062–1074 (2005).
 6. M. C. Lee and M. C. Wu, "Tunable coupling regimes of silicon microdisk resonators using MEMS actuators," *Opt. Express* **14**(11), 4703–4712 (2006).
 7. V. R. Almeida, Q. Xu, C. A. Barrios, and M. Lipson, "Guiding and confining light in void nanostructure," *Opt. Lett.* **29**(11), 1209–1211 (2004).
 8. N. K. Fontaine, J. Yang, Z. Pan, S. Chu, W. Chen, B. E. Little, and S. J. Ben Yoo, "Continuously tunable optical buffering at 40Gb/s for optical packet switching networks," *J. Lightwave Technol.* **26**(23), 3776–3783 (2008).
 9. M. L. Povinelli, M. Loncar, M. Ibanescu, E. J. Smythe, S. G. Johnson, F. Capasso, and J. D. Joannopoulos, "Evanescent-wave bonding between optical waveguides," *Opt. Lett.* **30**(22), 3042–3044 (2005).
 10. L. Martinez and M. Lipson, "High confinement suspended micro-ring resonators in silicon-on-insulator," *Opt. Express* **14**(13), 6259–6263 (2006).
-

1. Introduction

Optical buffering is a much-sought after function, both in packet-switched optical networks as well as in silicon photonics for optical processing on computer chips. The primary function of an optical buffer is to retain the data in its optical format during the desired storage time, without having to resort to OEO (optical-electronic-optical) conversion. To date, however, solutions for realizing this function are still somewhat limited.

In the simplest approach, fixed length optical delay lines are used, e.g. with discrete lengths of optical fiber [1]. A fixed delay, however, imposes undesirable restrictions on the flexibility of the optical buffer. Implementing a fixed delay line as part of a recirculating loop by incorporating an optical switch can yield delays that are multiples of the fundamental [1,2]. Additional delay choices can be obtained by having a number of different fiber lengths for the optical switch to select from; however, such configurations can quickly become unwieldy and bulky in practice as a means to achieving a quasi-variable buffer.

The use of optical resonators is another popular option, as they can produce significant delays in a very compact package [3]. Tunable optical buffers have also been demonstrated by using thermally phase-shifted ring resonators [4]. However, with resonators, there is a basic tradeoff between the amount of delay achievable and the useable optical bandwidth and hence

data capacity corresponding to that delay; resonators are essentially narrowband devices. Optical buffers based on slow light in electromagnetically induced optical media have also been suggested, but appear to have significant limitations on capacity and restrictions to the optical coherence time of the data signal [5].

In this paper, we propose a different approach for a continuously tunable optical buffer: a dual silicon waveguide where the propagation time delay can be varied considerably by mechanically changing the separation between the two waveguides.

2. Device configuration and results

The concept for the variable delay optical buffer is shown in Fig. 1. It consists of two silicon waveguides of height h and width w , coupled through an air gap d . The propagation delay is controlled by varying the distance d between the two waveguides, which can be achieved using MEMS techniques, such as electrostatic actuators [6]. We show that with such a configuration the waveguide propagation delay can be continuously changed several-fold by moving the waveguides towards each other. Even very small mechanical reconfiguration allows much larger optical changes than can be achieved by traditional electro-optic processes.

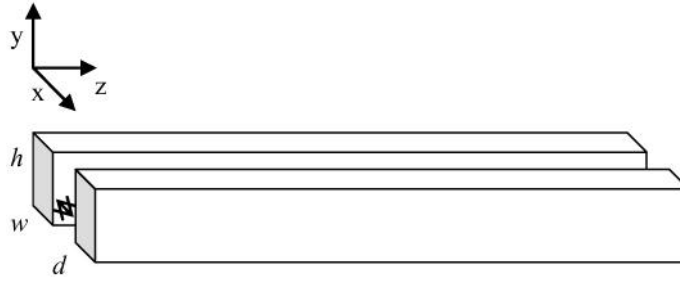


Fig. 1. Coupled silicon waveguides separated by distance d , with propagation delay varied through changing the separation.

The optical modes corresponding to the individual silicon waveguides far apart from each other, i.e. uncoupled, are the TE (transverse electric) and TM (transverse magnetic) modes, where TE refers to the electric field in the y -direction, i.e. along the major axis of the individual waveguides for $h > w$, and TM to the electric field along the x -direction. As the waveguides are moved closer together, but still far enough apart so that they are weakly coupled, the 4 lowest order modes of the combined structure are closely described by superpositions of the individual waveguide modes, i.e. symmetric and antisymmetric TE and TM modes, where the mode symmetry is with respect to the $x=0$ mirror plane. For the optical buffer, we will be concerned with just the symmetric TM and TE modes, as the antisymmetric modes are no longer supported when the gap becomes small enough.

Our numerical results are based on a fully vectorial finite element method (COMSOL Multiphysics®) to calculate the eigenmodes of the two-waveguide system, using a refractive index of silicon of 3.4. The calculations yield the effective phase index n_p as a function of wavelength λ , from which the group index n_g and the group velocity dispersion D are obtained by numerical differentiation as

$$n_g = n_p - \lambda \frac{\partial n_p}{\partial \lambda} \quad \text{and} \quad D = -\frac{\lambda}{c} \frac{\partial^2 n_p}{\partial \lambda^2}, \quad (1)$$

respectively. We first calculated the group index n_g for the x -polarized mode for very small ($d=0\text{nm}$) and very large ($d \rightarrow \infty$) waveguide separation as a function of width w and height h . The results show that the group velocity difference is maximized for waveguides with $h=300\text{nm}$ and $w=200\text{nm}$, dimensions that are not very different from silicon waveguides fabricated previously [3]. For this specific design, the group index (proportional to the

propagation time delay) and group velocity, as a function of the gap separation between the two silicon waveguides, are shown in Fig. 2 for both the symmetric TM (x-polarized) and TE (y-polarized) eigenmodes. It is seen that the largest change imparted to the propagation delay by changing the distance d is obtained with the symmetric TM eigenmode. Indeed, the delay time increases continuously by over 100% (3x, in fact) when the separation between the two waveguides changes by $\sim 500\text{nm}$. The calculations are shown for 3 wavelengths covering the $1500\text{nm} - 1600\text{nm}$ transmission window, showing that the device is potentially capable of supporting wideband WDM operation.

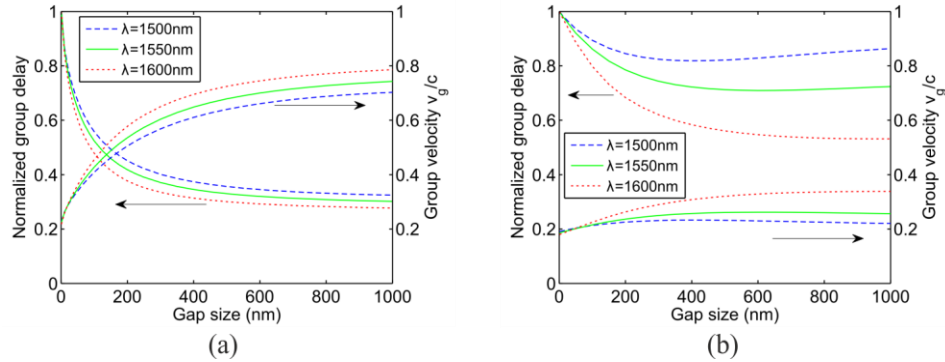


Fig. 2. Normalized propagation delay and group velocity for (a) the symmetric TM eigenmode and (b) the symmetric TE eigenmode of the dual silicon waveguide structure. Each waveguide has $h=300\text{nm}$, $w=200\text{nm}$.

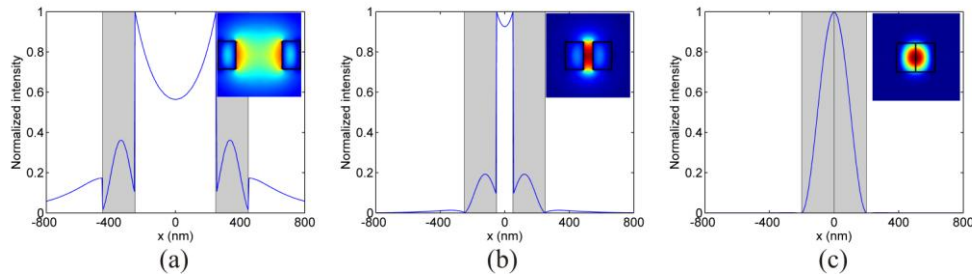


Fig. 3. Field intensity distribution of the TM mode (x-polarization) of the dual silicon waveguide structure for gap separations of (a) 500nm , (b) 100nm , and (c) 0nm at $\lambda=1550\text{nm}$. Shaded areas indicate the positions of the two waveguides. Insets in each graph show the equivalent color contour plots (red regions: high intensity, blue regions: low intensity).

Figure 3 shows the optical intensity of the symmetric superposition of TM eigenmodes (x-polarization) for the waveguide structure at various gap separations. The electric field is considerably enhanced in the gap between the two waveguides, which is a consequence of the boundary conditions for the electric field E_x at the silicon (high index)-air (low index) interface. In fact, for small gap distances (50nm), the dual waveguide structure may be analyzed as a slot waveguide, which has been of considerable research interest because of the high field intensities obtainable within the slot [7]. However, the underlying principle behind this tunable optical buffer is not reliant on obtaining high field intensities inside the slot. Similarly large changes in propagation delay can also be achieved using the symmetric TE eigenmode, with appropriate optimization of the silicon waveguide dimensions. The latter may be a useful practical option, as optical surface scattering losses associated with slot waveguides tend to be high due to the high field intensities at the air-silicon interface.

To show that the above results are equally applicable for the symmetric TE eigenmode, we present the calculations for waveguide dimensions of $h=300\text{nm}$, $w=140\text{nm}$. Here, the width w was changed compared to the geometry discussed above in order to maximize the group

velocity difference of this mode between the cases of narrow and wide waveguide separations. Figure 4 shows that the propagation delay changes more gradually with gap distance, but a similarly large (3x) continuous change is still obtained. However, the electric field intensity distributions show that the intensity in the gap is now considerably lower than in the previous (TM eigenmode) case.

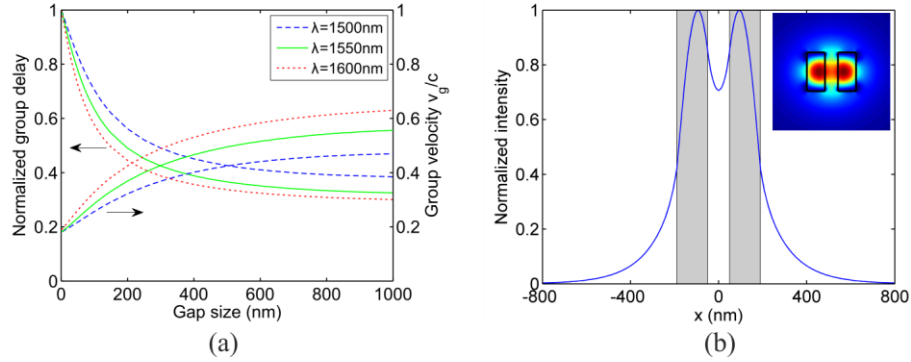


Fig. 4. (a) Normalized propagation delay and group velocity for the symmetric TE eigenmode (y-polarization) and (b) intensity profile for waveguide dimensions $h=140$ nm, $w=300$ nm, with a gap distance of 100nm at $\lambda=1550$ nm.

3. Discussion

From the results presented, the physical basis for the large change in the propagation delay in the dual silicon waveguide structure can be explained. The silicon waveguides are optimized such that, when the two waveguides are far apart, significant fractions of the optical field lie in the air, resulting in a low effective group index. When the two waveguides are brought together, the gap between them becomes small, and the two waveguides can effectively be viewed as one single (larger) waveguide, with the same height but twice the width. The net effect is that much of the light becomes captured within the larger silicon waveguide, with an accompanying large increase in the group index. As this underlying mechanism holds for both TE and TM modes, it is therefore a matter of optimizing the waveguide dimensions to maximize the change in propagation delay in each of the TM and TE cases.

The dispersion imparted by the structure is also of interest, as it could impose limitations to the bit rates/time delays achievable. The dispersion as a function of the gap distance is shown in Fig. 5. Figure 5(a) shows the dispersion behavior associated with the symmetric TM eigenmode, with the waveguide dimensions the same as that in Fig. 3. Figure 5(b) shows the dispersion associated with the symmetric TE eigenmode corresponding to the waveguide dimensions in Fig. 4.

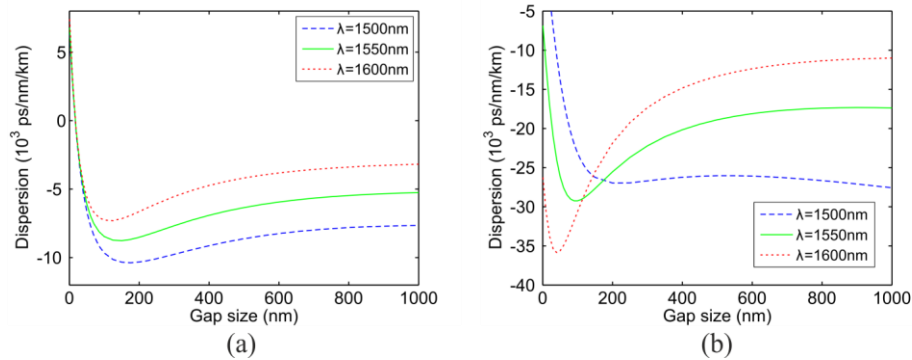


Fig. 5. Dispersion behavior for the symmetric (a) TM (waveguide as in Fig. 2) and (b) TE eigenmodes (waveguide as in Fig. 4).

We note that although the dispersion is not insignificant, on the order of 10^4 ps/nm/km, it would enable transmission of signals at 40Gb/s bit rates over waveguides of order a meter long without dispersion compensation. For more realistic integrated device lengths of 10cm with a corresponding tunable delay time of 1ns, the device dispersion amounts to ~ 1 ps/nm. By comparison, for the resonator-based optical buffer of Ref. [3], which employed silicon waveguides of a similar cross section and had a 510ps time delay, a group delay dispersion of 650ps/nm was measured, which limited the maximum bit rate to 15Gb/s. Thus, the achieved delay bit-rate product was 7.7, for signals within the narrow resonator bandwidth of 54GHz. A similar delay bit-rate product of 8.2 was also reported for tunable cascaded microring resonators in silica [8]. The tunable optical buffer proposed in this paper, on the other hand, has a useable bandwidth covering the whole C-band of telecommunication wavelengths; e.g. with a 10cm long device operating at 40Gb/s bit rates, the delay bit-rate product would be 40, a 5-fold improvement over the resonator approaches.

Our discussions have so far assumed perfectly straight and parallel waveguides. We note that the tight mode confinement in the silicon waveguides leads to a very short Rayleigh length of order $0.1\mu\text{m}$. Thus, the propagating light will follow adiabatically any bending or deformation in the waveguide geometry on a length scale longer than that. The overall device dispersion would then be given by averaging D over the local values.

In practice, such a dual waveguide buffer could be built from suspended silicon waveguides supported by silica pillars, similar to the structure shown in [9]. To ensure efficient coupling into the symmetric superposition mode, the ends of the two waveguides could be brought together at the device input and output by Y-junctions, allowing for low-loss coupling into and out of a single waveguide. Because of the above-mentioned adiabatic condition, mode coupling losses at the Y-junctions as well as at subsequent waveguide deformations, e.g. those introduced by mechanical actuation, would be negligible. We further note that for the specific designs discussed in Figs. 3 and 4, the asymmetric superposition modes are in fact beyond cutoff for waveguide separations smaller than $1\mu\text{m}$, and thus cannot be excited. Mechanical actuation of the waveguides could be achieved via electrostatic dipole forces without direct mechanical contacts to the waveguides [6], without incurring additional losses. Losses at the support structures required to keep the waveguides suspended can be as low as 0.2dB per suspension bridge, and can even be reduced to 0.02dB by appropriate tapered designs [10].

Finally, we note that optical forces can be exerted on the waveguides by the propagating signals themselves [9] to create a deflection in the gap distance, which may limit the signal power to $<10\text{mW}$. Alternatively, this deflection mechanism could be used to control the gap distance, by propagating an additional optical control beam through the waveguides as the actuator mechanism, instead of electrostatic forces.

4. Conclusion

We have proposed a continuously tunable optical buffer based on a dual silicon waveguide structure, with the two silicon waveguides separated by a gap of $1\mu\text{m}$ or less. Changing the gap distance produces a continuous change in the group index and propagation time through the waveguide structure. The device works with both TM and TE polarizations, but the waveguide dimensions should be optimized for the desired polarization in order to obtain the maximum change in the propagation delay.

Acknowledgments

This work was partly supported by EPSRC (Engineering and Physical Sciences Research Council) via a Programme Grant on the 'Photonic Hyperhighway' project, EP/I01196X/1.